UCLA UCLA Previously Published Works

Title

Analysis of thermocapacitive effects in electric double layers under a size modified mean field theory

Permalink https://escholarship.org/uc/item/2sn8d8tr

Journal Applied Physics Letters, 111(17)

ISSN 0003-6951

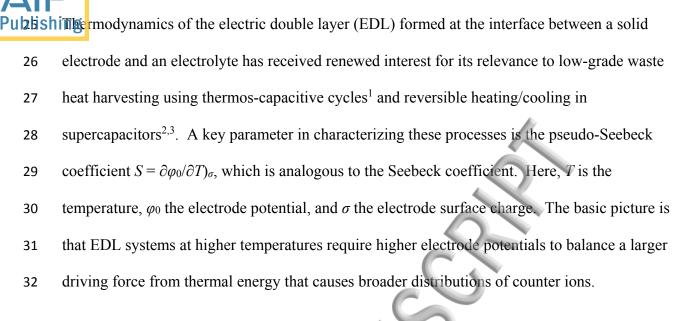
Author Ju, Y Sungtaek

Publication Date 2017-10-23

DOI 10.1063/1.5003362

Peer reviewed

Г						
		This manuscript was accepted by Appl. Phys. Lett. Click here to see the version of record.				
F		hing Analysis of Thermocapacitive Effects in Electric Double Layers				
² under a Size Modified Mean Field Theory						
	3					
	4					
	5	Y. Sungtaek Ju				
	6	University of California				
	7	420 Westwood Plaza, Los Angeles, CA 90095-1597, USA				
	, 8					
	9					
	10	Thermodynamics of the electric double layer (EDL) has received renewed interest for their				
	11	potential application in low-grade waste heat harvesting and reversible heating/cooling in				
	12	supercapacitors. We apply a size-modified mean field theory to analytically capture the				
	13	influence on the pseudo-Seebeck coefficient $S = \partial \varphi_0 / \partial T \rangle_\sigma$ of different factors, including the				
	14	electrode potential φ_0 , asymmetry in ion sizes and ion concentration, under a fixed electrode				
	15	surface charge σ . The pseudo-Seebeck coefficient is predicted to scale as φ_0/T at low electrode				
	16	potentials, but it reaches limiting values when the electrode potential exceeds crossover values				
	17	due to the steric effect. The qualitative behavior changes substantially, however, when the				
	18	temperature dependence of the permittivity is taken into account. The pseudo-Seebeck				
	19	coefficient S is then predicted to scale linearly with φ_0 even at high electrode potentials,				
	20	significantly over-predicting the experimental values. This suggests a strong influence of				
	21	phenomena not captured in the mean field theory, such as deviation of local effective				
	22	permittivity from the bulk value, thermally facilitated adsorption or desorption of ions on				
	23	electrode surfaces and weakening of ionic associations with temperature.				



33 Previous studies reported analytic expressions for the surface potential as a function of the temperature under the mean field theory for symmetric ions. Janssen et al.⁴ noted that the 34 pre-factor $k_{\rm B}T$ in the expression for φ_0 provides its predominant temperature dependence, 35 suggesting nearly temperature-independent S. This, however, is an incomplete picture. The 36 pseudo-Seebeck coefficient S is a function of the temperature and, as we shall show, the quasi-37 linearly temperature-dependence of ϕ_0 reported in the previous study, in fact, reflects dominant 38 influence of the temperature-dependence of permittivity rather than the intrinsic thermodynamics 39 of EDL. 40

In the present work, we use a size-modified mean field theory (SMFT) that extends the Korynshev-Kilic-Bazant-Ajdari mean field theory on a 1D flat surface⁵ to further examine the influence on *S* of the electrode potential, asymmetry in ion sizes, ion concentration and temperature-dependent permittivity. Although their deficiencies are well-known⁶, we employ the mean field theory in the hope of capturing analytically at least some qualitative features of the pseudo-Seebeck coefficient across a wide range of applied electrode potentials. This then

different phenomena occurring at the electrode-electrolyte interfaces.

We first describe derivation of the analytic expressions for *S*. Past studies^{5,7} used the lattice gas model to write the Helmholtz free energy in terms of the number of cations, anions, and available lattice sites and obtained potential-dependent ion concentrations in terms of modified Boltzmann distributions. These ionic concentrations were then used to express the charge density distribution ρ :

54
$$\rho_{SMFT}(u) = \left(\frac{2ec_0}{\gamma}\right) \frac{\exp(-u) - \exp(u) \left[\frac{\xi \exp(u) + \eta}{\xi + \eta}\right]^{\frac{1}{\xi} - 1}}{\exp(-u) + (\xi + \eta) \left[\frac{\xi \exp(u) + \eta}{\xi + \eta}\right]^{\frac{1}{\xi}}}$$
(1)

- Here, *u* is the dimensionless potential (= $e\varphi/k_BT$); γ is the packing parameter (= $2N_0/N$); ξ is the volume ratio between the anion and cation; η is the porosity (= $2/\gamma - 1 - \xi$); *N* is the total number of available lattice sites that can be occupied by cations; N_0 is the number of ions in the bulk; and *c*₀ is the ion concentration in the bulk.
- 59 We note that in the limit of high positive electrode potentials, Eq. (1) approaches
- $\rho \to -\frac{2ec_0}{\xi\gamma} \tag{2}$
- 61 In the limit of high negative electrode potentials, Eq. (1) approaches

$$\rho \to \frac{2ec_0}{\gamma}$$

The effect of this asymmetric behavior on *S* will be discussed later. The corresponding
expression for the charge density distribution under the Gouy-Chapman theory is

65

$$\rho_{GC}(u) = -2ec_0 \sinh(u) = -ec_0 [\exp(u) - \exp(-u)]$$
(4)

(3)



Equation (1) was substituted into the Poisson equation, which was solved to yield the expression for the electrode surface charge σ as a function of the dimensionless electrode potential u_0 :

$$70 \qquad \sigma(u_0)_{SMFT} = \operatorname{sgn}(u_0) \operatorname{ec}_0 L_D \sqrt{\frac{8}{\gamma}} \sqrt{\ln\left[\exp(-u_0) + (\xi + \eta)\left[\frac{\xi \exp(u_0) + \eta}{\xi + \eta}\right]^{\frac{1}{\xi}}\right] + \ln\left(\frac{\gamma}{2}\right)} \tag{5}$$

Note that φ represents the electric potential, which varies spatially across the EDL, whereas φ_0 represents the electric potential at the electrode. The corresponding expression under the Gouy-Chapman theory is

$$\sigma(u_0)_{GC} = 4ec_0 L_D \sinh\left(\frac{u_0}{2}\right) \tag{6}$$

75 The pre-factor in Eq. (5) is sometimes referred to as the crossover surface charge density σ^* :

76

74

$$\sigma^* = ec_0 L_D \sqrt{\frac{8}{\gamma}} \tag{7}$$

 σ^* can be interpreted as the surface charge density where the electrode potential becomes sufficiently large such that the ion concentration reaches the steric limit, causing the GC theory to deviate from the SMFT theory. The Debye length L_D is defined as

80
$$L_D = \sqrt{\frac{\varepsilon \varepsilon_0 k_B T}{2e^2 c_0}}$$
(8)

Equation (5) gives σ as a function of $u_0 (= e\varphi_0/k_BT)$. That is, the expression for $\sigma(\varphi_0, T)$ given above only implicitly relates φ_0 and T. We obtain the derivative $\partial \varphi_0 / \partial T \rangle_{\sigma}$ using the basic relation from the multi-variable calculus: This manuscript was accepted by Appl. Phys. Lett. Click here to see the version of record.



$$S = \frac{\partial \varphi_0}{\partial T} \Big|_{\sigma} = -\frac{\frac{\partial \sigma}{\partial T} \Big|_{\varphi_0}}{\frac{\partial \sigma}{\partial \varphi_0} \Big|_{T}} = \frac{\frac{\partial \sigma}{\partial T} \Big|_{\varphi_0}}{C_d}$$
(9)

The partial derivative $\frac{\partial \sigma}{\partial \varphi_0} \Big|_T$ may be recognized as the differential capacitance C_d . By taking the respective derivatives of Eq. (5) required for Eq. (9) and performing rather tedious algebraic manipulations, we obtain one of the key equations of the present work.

88
$$\frac{\partial \varphi_0}{\partial T} \Big)_{\sigma,SMFT} = \frac{\varphi_0}{T} + \frac{k_B}{e} \left(1 + \frac{T}{\varepsilon} \frac{d\varepsilon}{dT} \right) \frac{B \ln(B\gamma/2)}{D}$$
(10)

89 Here B and D are defined as

90
$$B = \exp(-u) + (\xi + \eta) \left[\frac{\xi \exp(u) + \eta}{\xi + \eta}\right]^{\frac{1}{\xi}}$$
(11)

91
$$D = \exp(-u) - \exp(u) \left[\frac{\xi \exp(u) + \eta}{\xi + \eta}\right]^{\frac{1}{\xi} - 1}$$
(12)

92 The corresponding expression under the Gouy-Chapman theory is

93
$$\frac{\partial \varphi_0}{\partial T}\Big)_{\sigma,GC} = \frac{\varphi_0}{T} - \frac{k_B}{2e} \left(1 + \frac{T}{\varepsilon} \frac{d\varepsilon}{dT}\right) \tanh\left(\frac{e\varphi_0}{k_BT}\right)$$
(13)

We first consider cases where the temperature dependence of the permittivity can be ignored ($d\varepsilon/dT$). Figure 1 shows the predicted *S* as a function of the electrode potential φ_0 for some representative values of the relevant parameters. The first terms on the right hand sides of Eqs. (10) and (13) are dominant under low electrode potentials. This can be understood as follows. In the absence of a steric limit on ion concentrations, maintaining the charge distribution ρ is in essence equivalent to keeping the exponent *u* in the Boltzmann distributions constant (Eq. (4)):



118

4

$$\frac{\partial}{\partial T} \left(\frac{\varphi}{T} \right) = 0 \quad \longrightarrow \quad S = \frac{\partial \varphi}{\partial T} = \frac{\varphi}{T}$$
(14)

102 This relation is approximate because the Debye length (and hence the spatial extent of the charge 103 density profile) itself is also a function of temperature. Nonetheless, for low electrode potentials, 104 $S = \partial \varphi_0 / \partial T \rangle_{\sigma}$ may be approximated by φ_0 / T under both the GC and SMFT theory.

High potential limits of S under the GC theory, however, are very different from those 105 under the SMFT theory. Under the GC theory, S can still well-approximated by φ_0/T . In 106 contrast, under the SMFT theory, S reaches limiting values at high (negative or positive) 107 potentials. This can be understood as follows. Because the charge density is limited by the 108 steric effects, an increase in temperature does not affect the charge density distribution near the 109 electrode surface where the magnitude of the electric potential is larger than crossover values 110 $[\ln(2/\xi\gamma) (k_BT/e)$ for positive potentials and $-\ln(2/\gamma) (k_BT/e)$ for negative potentials]. An increase 111 in temperature then would only affect the charge density distribution away from the electrode 112 surface where the magnitude of the electric potential is lower. As a result, there is no longer 113 commensurate changes in S. 114

In the limit of large positive electrode potentials and $\eta \gg \xi$, Eq. (5) can be approximated by ignoring the term exp(- u_0). The electrode potential can then be expressed as an explicit function of the electrode surface charge:

$$\varphi_0 = -\left(\frac{\xi}{e}\right) k_B T \ln\left[\frac{\eta \gamma\left(\frac{\xi}{\eta}\right)^{\frac{1}{\xi}}}{2}\right] + \frac{\sigma^2 \xi \gamma}{4ec_0 \varepsilon \varepsilon_0}$$
(15)

h



Publishinghis limit, the electrode potential is a linear function of T. Its derivative S becomes

120 independent of both the electrode potential and the temperature. It depends only on the ion size

121 ratio ξ and the packing factor γ :

122
$$\frac{\partial \varphi}{\partial T} \Big)_{\sigma, SMFT, \varphi \to +\infty} \approx -\frac{\xi k_B}{e} \ln \left[\frac{\eta \gamma(\xi/\eta)^{\frac{1}{\xi}}}{2} \right]$$
(16)

123 Using a similar procedure, we can also find *S* in the limit of large negative potentials:

124
$$\frac{\partial \varphi_0}{\partial T} \Big)_{\sigma, SMFT, \varphi_0 \to -\infty} \approx \frac{k_B}{e} \ln \left[\frac{\gamma}{2} \right]$$
(17)

These different limiting behaviors under the positive and negative electrode potentials for electrolytes containing asymmetric ions are expected from the difference between Eqs. (2) and (3). When anions are smaller than cations ($\zeta < 1$), as an example, the maximum allowed density of anions (at the positive electrode) exceeds that of cations (at the negative electrode). The GC theory and its predicted linear dependence of *S* on φ_0 therefore holds to higher values of φ_0 at the positive electrode interface than at the negative electrode interface. The limiting value of *S* for large positive potentials would therefore be larger than that for large negative potentials.

Figure 2 shows the limiting values of *S* for large positive electrode potential (Eq. (16)) as a function of the packing parameter γ (i.e. bulk electrolyte ion concentration) for two different values of ξ . By allowing anions to achieve higher sterically-limited concentrations, the smaller value of ξ leads to larger values of *S*_{limit}. For both cases, *S*_{limit} decreases with increasing packing parameter γ and hence increasing bulk ion concentration.

137 So far, our discussion assumed that the permittivity is independent of temperature. In reality,138 the permittivity of a solvent, notably water, is itself a function of temperature. Note that our

Publishide vation for *S*, as expressed in Eq. (10), does account for this temperature-dependence of permittivity albeit under the mean field approximation of position-independent permittivity.

The term (*T*/ε) (*dε/dT*) in Eq. (10) can have a magnitude of the order of 1 in some
solvents (e.g., approximately -1.35 for pure water at room temperature) and the temperature
dependence of the permittivity may completely dominate the general behavior of *S*. In this case,
Eq. (10) may be approximated in the limit of high electrode potentials as:

145
$$\frac{\partial \varphi_0}{\partial T} \Big|_{\sigma, SMFT, |\varphi_0| \to \infty} \approx -\left(\frac{T}{\varepsilon} \frac{d\varepsilon}{dT}\right) \frac{\varphi_0}{T} = -\left(\frac{1}{\varepsilon} \frac{d\varepsilon}{dT}\right) \varphi_0 \tag{18}$$

146 That is, the predicted *S* continues to increase approximately linearly with φ_0 even at high 147 electrode potentials for non-zero $d\varepsilon/dT$. In fact, the magnitudes of *S* predicted may significantly 148 exceed the limiting values calculated from Eq. (16) or Eq. (17) as illustrated in Figure 3.

For typical temperature ranges of practical interest, ε of common solvents varies nearly linearly with temperature and $d\varepsilon/dT$ can be assumed constant. Equation (18) then predicts *S* to be nearly independent of temperature, consistent with the quasi-linear temperature dependence of φ_0 predicted in the previous study⁴. We would like to emphasize again that this result reflects the dominant influence of the temperature-dependent permittivity rather than the intrinsic thermodynamics of EDL captured in the MFT theory.

Experimental values of *S* reported in the literature from commercial supercapacitors were approximately 0.5 mV/K at a starting electrode potential of 2.5 V¹. This is comparable to the limiting values of 0.1 ~ 0.4 mV/K predicted from Eq. (16) but much smaller than values of the order of 10 mV/K predicted from Eq. (18) ($\gamma = 0.1 \sim 0.5$; $\xi = 0.1 \sim 1$; $\varepsilon = 50$; $d\varepsilon/dT = 0.2$ K⁻¹).



The electric double layer (EDL) structure is often complicated by multiple factors, such as various conformations of ions, ionic correlations, specific adsorption and electrode 161 morphology. The large discrepancy between the experimentally measured values of S and the 162 prediction from Eq. (10) or Eq. (19) may be explained by one or more of these factors. In fact, 163 some of these factors were suggested as causing the increase in capacitance with increasing 164 temperature despite decreasing solvent permittivity. Such anomaly, observed experimentally but 165 not captured by the current SMFT theory, may also be responsible for the diminished magnitude 166 of S. Recall that the differential capacitance is in the denominator of the expression for S in Eq. 167 (9). Another possibility is that local permittivity is influenced strongly by large local electric 168 fields⁸, which then greatly suppresses the temperature dependence of the effective permittivity in 169 the EDL. 170

As we alluded to, previous studies^{9,10} reported that the differential capacitance of EDL 171 capacitors may increase with temperature, in direct contrast to the prediction of traditional 172 models. Some past studies often attributed this positive temperature dependence to the 173 weakening of ionic association at increased temperatures, which leads to more effective 174 screening of the electrode potential. Another study¹¹ argued instead that decrease in electrolyte 175 viscosity with increasing temperature promotes adsorption of counter ions in electrode pores and 176 is thus responsible for the increase in capacitance. Still other studies, focused on ionic liquids¹², 177 considered competition between two phenomena: 1) overall thickening of the EDL with 178 increasing thermal energy and 2) weakening of specific adsorption of co-ions on an electrode. 179 The latter would enable relatively higher packing of counter-ions and thereby more effective 180 screening of the electrode than otherwise expected. One may then postulate that the reduced 181



Publishing if it adsorption of co-ions at an increased temperature counteracts a reduction in capacitance accompanying the decrease in permittivity.

Related to this discussion are experimental observations^{13,14} of thermodiffusion in 184 aqueous suspensions of nano- and micro-scale solid particles. When interpreted using existing 185 theoretical models of the thermodiffusion coefficient, the experimental data suggested that 186 $(T/\varepsilon)(d\varepsilon/dT)$ vary substantially with temperature, changing signs and reaching values as high as 187 +2.44 for aqueous suspensions of polymer particles at room temperature.¹⁴ This value marks a 188 stark departure from the negative value of -1.4 for bulk water, commonly used in previous 189 studies.¹³ When averaged over certain temperature windows, the positive contribution of 190 $(T/\varepsilon)(d\varepsilon/dT)$ from one temperature region may then cancel out the negative contribution from 191 192 another temperature region.

The current SMFT theory also does not capture the formation of ordered structures in 193 electrolytes at the electrode interface, such as a multilayer structure described by exponentially 194 decaying sinusoidal oscillations in ion densities perpendicular to the interface, and associated 195 over-screening effects. Unlike the Debye length, the period and magnitude of these oscillations 196 were predicted to decrease with increasing temperature in molecular dynamic simulation of 197 EDLs of a molten salt¹⁵. At high electrode potentials, however, a previous study using a Landau-198 Ginzburg-type continuum theory of solvent-free ionic liquids¹⁶ reported that over-screening from 199 short-range correlations is suppressed in favor of steric constraint-induced crowding of counter 200 ions near the electrode. 201

In summary, we apply a size-modified mean field theory to analytically capture the influence of different factors on the pseudo-Seebeck coefficient $S = \partial \varphi_0 / \partial T \rangle_{\sigma}$. We derive



Publishing ytic expressions of S and show that it scales as φ_0/T at low electrode potentials but reaches

- 205 limiting values when the electrode potential exceeds crossover values due to the steric effect.
- 206 The temperature dependence of the permittivity, however, can significantly modify this behavior.
- For appreciable values of $d\varepsilon/dT$, the parameter S is predicted to scale linearly with φ_0 even at
- 208 high electrode potentials, significantly over-predicting the experimental values. Our work
- 209 motivates further experimental and theoretical studies to elucidate the effects of phenomena
- 210 hitherto not captured under the SMFT theory on the pseudo-Seebeck coefficient.
- 211
- 212

Acknowledgment

214

Publishing

- DOF ARPA -E under grant DE-~ • . • ~ 215 216
- 217
- 218

AR0000532.	based in part or	n work perform	ed with support	trom DOE ARPA-E
			S N	
P C C C				



References

220

- ¹ A. Härtel, M. Janssen, D. Weingarth, V. Presser, and R. van Roij, Energy Environ. Sci. 8, 2396 (2015).
- ²J. Schiffer, D. Linzen, and D.U. Sauer, J. Power Sources **160**, 765 (2006).
- ³ M. Janssen and R. van Roij, Phys. Rev. Lett. **118**, 096001 (2017).
- ⁴ M. Janssen, A. Härtel, and R. van Roij, Phys. Rev. Lett. **113**, 268501 (2014).
- ⁵ Y. Han, S. Huang, and T. Yan, J. Phys. Condens. Matter **26**, 284103 (2014).
- ⁶ M.S. Kilic, M.Z. Bazant, and A. Ajdari, Phys. Rev. E **75**, 021502 (2007).
- ⁷ V.B. Chu, Y. Bai, J. Lipfert, D. Herschlag, and S. Doniach, Biophys. J. **93**, 3202 (2007).
- ⁸ J.O. Bockris, M.A.V. Devanathan, and K. Müller, Proc. R. Soc. Lond. A 274, 55 (1963).
- ⁹ V. Lockett, R. Sedev, J. Ralston, M. Horne, and T. Rodopoulos, J. Phys. Chem. C 112, 7486 (2008).
- 232 ¹⁰ S.A. Kislenko, R.H. Amirov, and I.S. Samoylov, Phys. Chem. Chem. Phys. **12**, 11245 (2010).
- ¹¹ M. Taniguchi, D. Tashima, and M. Otsubo, in 2007 Annu. Rep. Conf. Electr. Insul. Dielectr.
- 234 *Phenom.* (2007), pp. 396–399.
- ¹² X. Liu, Y. Han, and T. Yan, Chem. Phys. Chem. **15**, 2503 (2014).
- ¹³ S.A. Putnam, D.G. Cahill, and G.C.L. Wong, Langmuir **23**, 9221 (2007).
- ¹⁴ L. Lin, X. Peng, Z. Mao, X. Wei, C. Xie, and Y. Zheng, Lab. Chip **17**, 3061 (2017).
- ¹⁵ J. Vatamanu, O. Borodin, and G.D. Smith, Phys. Chem. Chem. Phys. **12**, 170 (2009).
- ¹⁶ M.Z. Bazant, B.D. Storey, and A.A. Kornyshev, Phys. Rev. Lett. **106**, 046102 (2011).
- 240





List of Figures

- 243 Figure 1 (color online) The predicted pseudo-Seebeck coefficient S as a function of the (initial) electrode potential. The solid line corresponds to the prediction from the GC theory and the 244 dashed and dash-dot lines from the SMFT theory for two different values of ξ . 245 246 Figure 2 (color online): The limiting (or saturation) values of S for large positive electrode 247 potentials as a function of packing parameter γ . The solid symbols correspond to predictions 248 from the full equation (Eq. (10)) and the hollow symbols from the approximate expression (Eq. 249 (16)). Two sets of results for two different values of ξ are shown. 250 251 Figure 3 (color online): The predicted values of S under the SMFT theory (Eq. (10)) for different 252
- values of $d\epsilon/dT$, illustrating the dominating influence of the temperature dependence of the
- 254 permittivity.

